ISSN: 2472-3703 DOI: 10.6911/WSRJ.202605_12(5).0006

Optimization Design of Wind Environment in Commercial Pedestrian Streets Based on Field Measurement and Numerical Simulation

Yurong Li[1], Zhonggou Chen[1, *], Guoyi Zhang[1, *]

[1]Department of Landscape and Architecture, Zhejiang A&F University, Hangzhou, China

[*] Corresponding author

Abstract

Taking the core area of Hangzhou Hubin Pedestrian Street as the study subject, this research comprehensively adopts field measurements and CFD numerical simulation to evaluate the existing wind environment and carry out zoned greening layout optimization. The model accuracy is validated as good through field measurements. The existing wind environment exhibits two types of problems: strong wind discomfort zones in the middle section of the main street, and stagnant wind zones on the leeward sides of buildings. Differentiated greening strategies are proposed for seven zones (A-G). After optimization, the green coverage rate of the street area increases from 1.70% to 5.90%, and the proportion of the ideal wind speed range (1.04-5.00 m/s) increases by 9.76 percentage points, among which the proportion of the 1.04-3.40 m/s range increases significantly, while the proportion of the uncomfortable wind speed range (5.01-10.7 m/s) decreases by 9.08 percentage points. The study shows that refined greening layouts based on zoning characteristics can effectively improve the wind environment of commercial pedestrian streets.

Keywords

Commercial pedestrian street; wind environment; greening layout; pedestrian wind comfort; CFD.

1. INTRODUCTION

Commercial pedestrian streets are the core carriers of public life in modern cities, and their microclimatic conditions directly determine users' comfort and willingness to stay [1, 2]. Rapid urbanization has weakened the natural ventilation capacity of cities and exacerbated the urban heat island effect [3]. How to actively optimize the wind environment of commercial pedestrian streets through design has become a key scientific issue for improving urban livability and sustainability.

Greenery, especially trees, can regulate the microclimate through canopy shading, transpiration, and the obstruction and guidance of airflow [4, 5]. Existing studies have clarified the fundamental effects of geometric elements such as building morphology, street aspect ratio, building layout, and spatial orientation on the flow field structure of street blocks [6-9], as well as the influence of greening parameters such as tree planting density, arrangement pattern, and canopy characteristics on the wind environment [10-12]. In recent years, research on the dynamic response of vegetation has begun to focus on real-time interactions between plants and wind fields [13], suggesting that greenery should be regarded as an active, context-dependent regulator rather than a passive static element.

ISSN: 2472-3703 DOI: 10.6911/WSRJ.202605_12(5).0006

2. METHODS

2.1. Control Equation

In this study, the air medium within the flow domain is treated as an incompressible ideal gas, and Phoenics—a mature and effective tool for investigating urban-scale wind environment problems—is selected as the simulation platform. The governing equations of the relevant k-ε turbulence model are given as follows:

$$\frac{\partial}{\partial t}(\rho k)+\frac{\partial}{\partial x_i}(\rho k u_i)=\frac{\partial}{\partial x_j}\left[\left(\mu+\frac{\mu_t}{\sigma_k}\right)\frac{\partial k}{\partial x_j}\right]+G_k+G_b-\rho\varepsilon-Y_M+S_k \tag{1}$$

$$\frac{\partial}{\partial t}(\rho \varepsilon)+\frac{\partial}{\partial x_i}(\rho k u_i)=\frac{\partial}{\partial x_i}\left[\left(\mu+\frac{\mu_t}{\sigma_\varepsilon}\right)\frac{\partial \varepsilon}{\partial x_j}\right]+C_{1\varepsilon}\frac{\varepsilon}{k}(G_k+c_{3\varepsilon}G_b)-C_{2\varepsilon}\rho\frac{\varepsilon^2}{k}+S_\varepsilon \tag{2}$$

where G_k is the generation term of turbulent kinetic energy due to mean velocity gradients; G_b is the generation term of turbulent kinetic energy due to buoyancy; Y_M represents the contribution of fluctuating dilatation to the overall dissipation rate in compressible turbulence; $C_{1\varepsilon}$, $C_{2\varepsilon}$, and $C_{3\varepsilon}$ are constants; σ_k and σ_ε are the turbulent Prandtl numbers for turbulent kinetic energy and turbulent dissipation rate, respectively; S_k is a user-defined source term for turbulent kinetic energy; and μ_t denotes the turbulent viscosity.

2.2. Study Wind Direction

Based on the meteorological observation data of Hangzhou, compiled and presented as Figure 1, after excluding extreme wind speeds, the maximum wind speed in summer (June to August) reaches 8 m/s, occurring across multiple time periods within the summer season. Therefore, this study adopts 8 m/s as the inlet wind speed parameter for numerical simulation. According to the hourly wind rose diagram from the relevant local standards of Zhejiang Province, the most frequent wind direction in Hangzhou during July is south-southwest (SSW), followed by southwest (SW), and then south (S). Accordingly, this paper adopts a simplified assumption of a single prevailing wind direction—south-southwest (SSW)—for the optimization design analysis of the wind environment of the commercial pedestrian street.

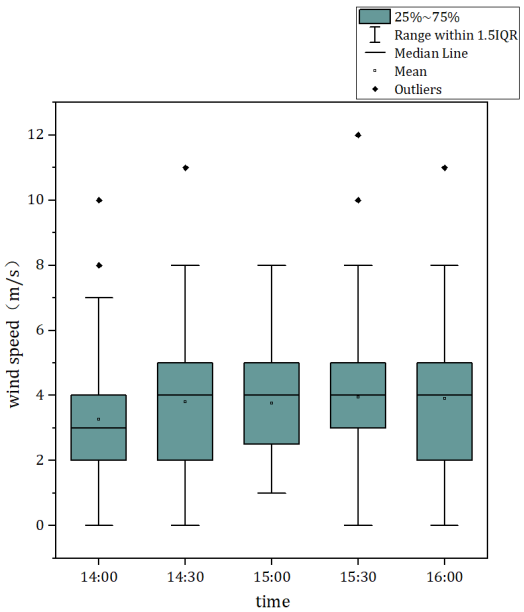

Figure 1. Statistical characteristics of wind speed at specific times in summer

ISSN: 2472-3703 DOI: 10.6911/WSRJ.202605_12(5).0006

2.3. Evaluation Indicators

This study selects the horizontal wind field at a height of 1.5 m above ground (the pedestrian breathing zone) as the evaluation object. The core evaluation metric is the proportion of area with ideal wind speeds. The ideal wind speed range is defined as $1.04\ m/s \leq V \leq 5.00\ m/s$ [14, 15]. Within this range, three sub-ranges are further defined, corresponding to common activity types in commercial pedestrian streets [16]: 1.04-2.10 m/s for prolonged sitting or standing, 2.11-3.40 m/s for short-term sitting or standing, and 3.41-5.00 m/s for walking [17].

3. FIELD MEASUREMENT AND SIMULATION VALIDATION

Hangzhou Hubin Pedestrian Street is located in the Hubin commercial area, the core business district of Hangzhou, adjacent to the eastern shore of the West Lake, a UNESCO World Heritage Site. It is an urban landmark block integrating commerce, leisure, tourism, and culture. At the end of 2018, Hubin Pedestrian Street became one of the first pilot projects for the renovation and upgrading of pedestrian streets nationwide, and in the following years, it was selected as one of the first national demonstration pedestrian streets.

In terms of spatial morphology, Hubin Pedestrian Street consists of multiple block units. The block has a clear spatial hierarchy, including main streets, secondary streets, plaza nodes, and rooftop terraces, providing diverse spatial experiences for crowd circulation, resting, and social interaction. Hubin Pedestrian Street has a certain greening foundation, with an overall layout combining points, lines, and areas, including street trees, vertical greenery, and rooftop gardens, which not only enhance landscape quality but also significantly influence the local microclimate.

As a high-quality commercial pedestrian street prioritized by Hangzhou, Hubin Pedestrian Street functionally accommodates high-density pedestrian flow, intensive commercial activities, and frequent public events, exhibiting typical thermal and wind environment sensitivity of urban central areas. With the advancement of urban renewal and quality improvement projects, the block has undergone systematic renovations in spatial morphology optimization, greening system restructuring, and public space revitalization, providing an ideal research carrier for this study.

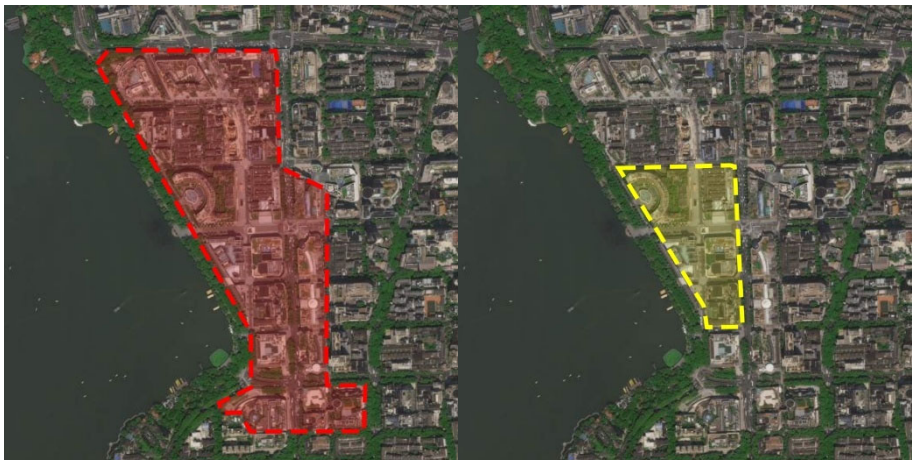

Figure 2. Satellite image of the overall scope and optimization sections of Hubin Pedestrian Street

Taking the core section of Hubin Pedestrian Street as the case study, field measurements were initiated on the afternoon of July 7, 2025. The wind direction on that day was east, with a wind force of Beaufort Scale 3. A total of 42 monitoring points were set up as shown in Figure

ISSN: 2472-3703 DOI: 10.6911/WSRJ.202605_12(5).0006

3, with a recording duration of 3 minutes at each point. The obtained data are summarized in Table 1.

Structured grids were used for the simulation, with refinement in areas containing buildings and trees. The computational domain was set to 740 m × 1160 m × 210 m, with a grid division of 393 × 504 × 67, resulting in a total of 13.27 million grid cells. The inlet boundary condition was defined using a power-law exponent function. Meteorological conditions were based on the data recorded on the measurement day, while other parameters were set to default values. Buildings and the ground were set as no-slip walls. Building shapes were simplified as rectangular blocks, with facade details omitted. The tree model uniformly adopted the average tree height and crown base height within the survey range as the vegetation-level variables. The number of simulation iterations was 1000. The simulation results are presented in Figure 4.

Figure 3. Monitoring point locations

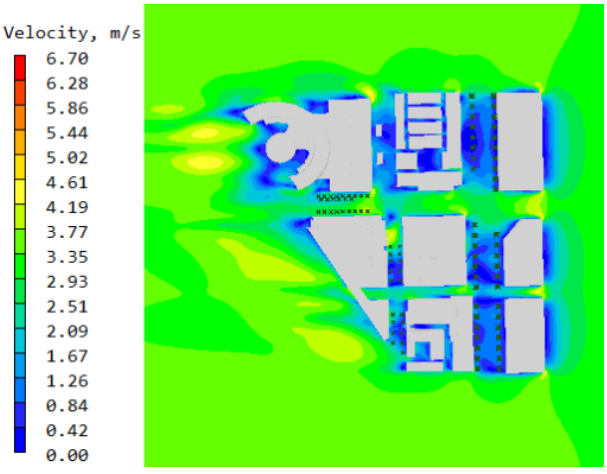

Figure 4. Wind speed contour map at 4.5 m height

In wind environment simulation studies, if the mean absolute percentage error (MAPE) is below 20% and the root mean square error (RMSE) is less than 0.20 m/s, the simulation results are generally considered acceptable. The comparison between simulation and measurement is summarized in Table 1 and Figure 5. The MAPE is 12.20%, and the RMSE is 0.19 m/s, both meeting the requirements, with the wind speed trend generally consistent.

ISSN: 2472-3703 DOI: 10.6911/WSRJ.202605_12(5).0006

Table 1. Comparison of simulated and measured wind speeds and corresponding errors

Monitoring point	Measured value	Simulated value	Error (X, %)	Monitoring point	Measured value	Simulated value	Error (X, %)
A1	2.68	2.71	0.99	**H1**	0.95	0.81	0.14
A2	2.89	3.13	8.29	**H2**	0.67	0.40	0.27
A3	3.49	3.56	2.14	**H3**	0.42	0.50	0.08
B1	2.25	2.35	4.44	**I1**	1.07	1.05	0.02
B2	2.89	3.06	5.75	**I2**	1.11	1.41	0.30
B3	1.96	2.22	13.46	**I3**	1.38	1.01	0.37
C1	1.54	1.68	9.39	**J1**	3.83	4.08	0.25
C2	2.27	2.31	1.70	**J2**	3.56	3.78	0.22
C3	1.51	1.78	18.11	**J3**	2.42	2.27	0.15
D1	4.28	4.42	3.36	**K1**	0.70	0.34	0.36
D2	3.51	3.84	0.78	**K2**	0.39	0.59	0.20
D3	3.13	3.27	4.42	**K3**	0.92	0.81	0.11
E1	2.68	2.88	7.62	**L1**	1.31	1.44	0.13
E2	2.64	2.47	6.37	**L2**	1.94	2.06	0.12
E3	2.75	2.46	10.72	**L3**	2.24	2.30	0.06
F1	2.53	2.48	2.13	**M1**	1.30	1.48	0.18
F2	2.51	2.40	4.31	**M2**	1.13	0.90	0.23
F3	2.66	2.43	8.49	**M3**	0.65	0.38	0.27
G1	4.32	4.51	4.44	**O1**	1.67	1.78	0.11
G2	2.39	2.40	5.37	**O2**	2.30	2.47	0.17
G3	1.76	1.73	1.70	**O3**	1.74	1.98	0.24

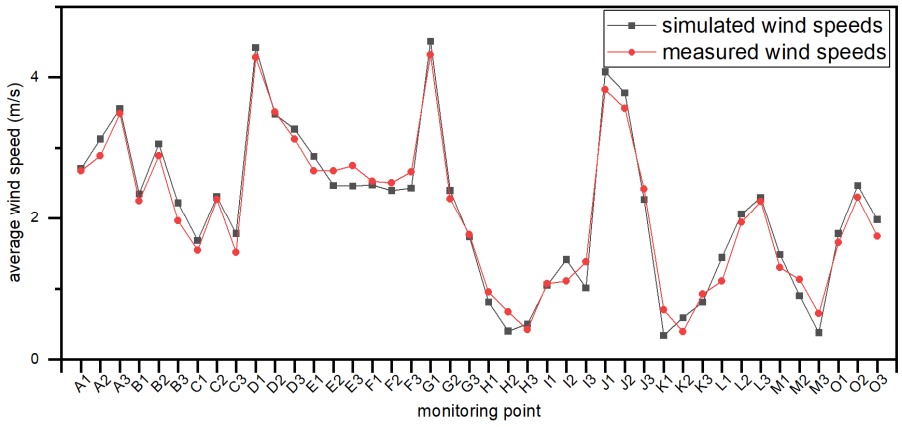

Figure 5. Comparison of simulated and measured wind speeds

4. RESULTS AND DISCUSSION

4.1. Simulation of Current Wind Environment and Identified Problems

As of the survey date, the core area of Hubin Pedestrian Street had relatively limited greenery. At the pedestrian breathing height of 1.5 m, trees have a greater influence on the wind environment than shrubs and grass [18]. Therefore, in this study, only trees are considered for analysis and optimization. A parametric model was established for numerical simulation, with the reference height wind speed set to 8 m/s and the prevailing wind direction being the summer south-southwest (SSW). To facilitate convergence, medium-sized trees were simplified as cubes with a canopy size of 4 m × 4 m × 4 m and a tree height of 7 m, while small

ISSN: 2472-3703 DOI: 10.6911/WSRJ.202605_12(5).0006

trees were simplified as cubes with a canopy size of 2.5 m × 2.5 m × 2.5 m and a tree height of 4 m. The resulting wind speed contour map is shown in Figure 6.

From the wind speed contour map at the pedestrian breathing height of 1.5 m, it can be seen that driven by the SSW incoming flow, airflow enters the site from the southwest side of the block, and a street canyon effect is formed along the longitudinal main pedestrian path that runs through the block. The continuous commercial buildings on both sides of the road form a stable airflow boundary. As the airflow enters the road, the flow cross-section significantly contracts, creating a continuous high-wind-speed zone along the road alignment. Among them, the middle section of the main road is the peak wind speed zone, while the wind speed in the northeastern section gradually decreases as the airflow diffuses. In contrast, areas such as branch pedestrian passages and street corner nodes on both sides of the main road experience reduced wind speeds due to building obstruction and flow separation around obstacles. The wind environment discomfort zones in the wind speed contour map can be mainly classified into two types: the strong wind discomfort zone in the middle section of the longitudinal main pedestrian street, and the stagnant wind zone in the eastern section of the north-south main pedestrian street.

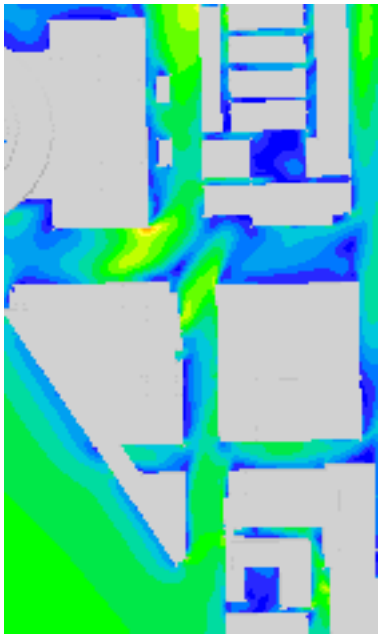

Figure 6. Simulated results at 1.5 m height

The strong wind discomfort zone is most significantly affected by the street canyon effect. When the SSW incoming flow enters the block, it encounters the turbulent flow at the intersection and is influenced by the surrounding buildings, forming two corner flow zones with wind speeds markedly different from the surrounding areas. The wind speeds in these zones are generally too high, compromising pedestrian wind comfort. This area constitutes the core pedestrian thoroughfare of the block, where high-frequency pedestrian activities combined with persistently high wind speeds can degrade the walking experience. It is therefore the key control zone for wind environment optimization within this block.

The eastern section of the north-south main pedestrian street is sheltered by building masses, forming a wind shadow zone. The southwesterly incoming flow struggles to reach this area directly, and after flowing around the buildings, its kinetic energy is substantially reduced, resulting in generally low wind speeds. Such zones suffer from severely inadequate natural

ISSN: 2472-3703 DOI: 10.6911/WSRJ.202605_12(5).0006

ventilation, making them prone to hot air stagnation in summer, which exacerbates the urban heat island effect within the block. Moreover, poor ventilation hinders the dispersion and dilution of pollutants, potentially leading to localized deterioration of air quality. Targeted optimization designs are therefore necessary to improve ventilation conditions.

4.2. Optimization Experiment Design

To facilitate refined analysis and comparison across different spatial locations, the commercial pedestrian street block is divided into seven zones (A to G) based on spatial morphology, as shown in the figure below. In the studied commercial pedestrian street, there are extensive impervious underlying surface types within the block, including individual buildings, paved roads, and plazas—such as concrete pavements, stone ground surfaces, and various artificial structures. As a result, the proportion of buildings and hard pavement in the urban underlying surface is excessively high, while the proportion of greenery is relatively low. Therefore, on the basis of increasing the green coverage rate, differentiated greening layout strategies are introduced in a targeted manner to improve the overall wind environment of the block and enhance pedestrian comfort.

In Zone A, there is no existing vegetation layout, and pedestrian traffic is heavy on both sides. There are two one-story commercial buildings added later in the street, and this zone contains a relatively high wind speed area. Under conditions where natural wind cannot be continuously and stably delivered, frequent gusts make the wind environment poor. Therefore, a single-row planting of medium-sized trees on the east side and partial row planting on the west side are adopted. The partial row planting on the west side takes into account the interference of trees with the two one-story buildings and the occupation of the passageways between west-side buildings after row planting.

Zone B is one of the main passages for the incoming wind direction entering the block. It contains a strong wind zone formed by both a building corner flow zone and a turbulent flow zone. The wind environment in Zone B directly affects the subsequent airflow through the block. Moreover, Zone B directly faces West Lake, so considering landscape factors, strategies such as central row planting that would obstruct the main sightline cannot be adopted. The existing ginkgo trees in this zone are growing poorly with small crown widths and cannot effectively dissipate wind energy through obstruction. Hence, two-sided row planting is adopted to replace the vegetation in the strong wind zone on the east side of Zone B, while the ginkgo trees on the west side are retained.

Zone C is the central area of the block and an intersection, where tree planting is not appropriate. Therefore, no layout strategy is introduced.

Zone D is not only a major entrance from the east-side urban road into Hubin Pedestrian Street and the West Lake Scenic Area, but also one of the entrances/exits of Longxiangqiao Station, a high-ridership metro line station. Thus, pedestrian volume is generally high. Additionally, the building on the north side of Zone D houses one of the high-traffic Apple flagship stores, and its street-facing facade is mainly composed of glass. Planting trees on this side would not only cause some inconvenience to pedestrians but also affect sightlines for both the interior and exterior of the building. In terms of the wind speed field, most of Zone D falls within a comfortable wind speed range suitable for pedestrians. After comprehensive consideration, no tree-based greening layout strategy is introduced in this zone.

Zone E has a narrower street cross-section than the aforementioned zones, and there are already some existing plants. From the wind speed field, a strong wind zone exists at the northern end of Zone E. However, a large commercial electronic display screen is located there, and planting trees would affect the overall landscape effect. Therefore, no layout is introduced

ISSN: 2472-3703 DOI: 10.6911/WSRJ.202605_12(5).0006

at that location. For the remaining parts of Zone E, additional row planting is added to the existing trees to increase the green coverage ratio.

Zone F is an east-west oriented street. After the incoming flow enters the street, a lateral wind zone with slightly higher wind speed than the surroundings is generated on the north side of the street, while the wind speed on the south side is relatively low. Therefore, single-row planting of small trees on the north side is adopted in this zone.

Zone G is also one of the main passages for incoming wind into the block, so its wind speed is higher than adjacent areas. Currently, only a few plants are arranged there. Hence, two-sided row planting of small trees identical to the existing species is adopted to control the wind speed range in this zone.

The three-dimensional optimized model of the entire block is shown in Figure 8. In this model, the portions rendered in green represent the additionally added tree models after optimization compared to the current situation.

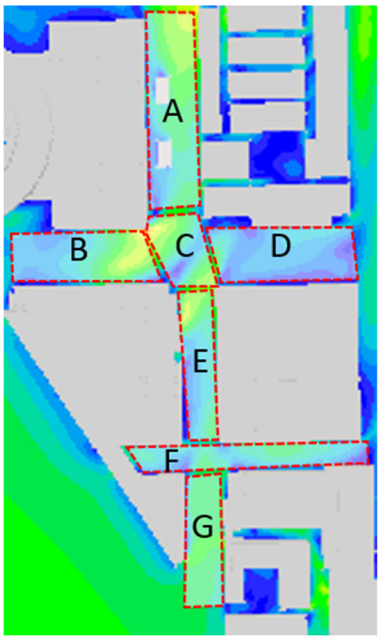

Figure 7. Zoning diagram

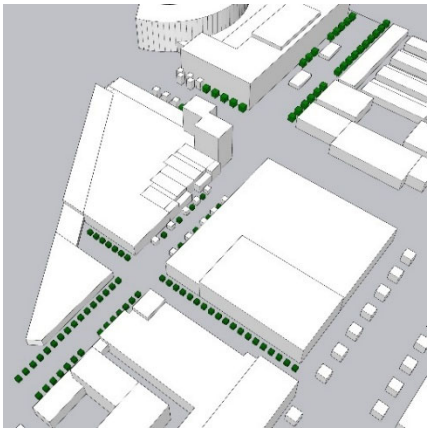

Figure 8. Schematic of the optimized model

ISSN: 2472-3703 DOI: 10.6911/WSRJ.202605_12(5).0006

4.3. Numerical Simulation Results and Indicator Analysis After Optimization

After importing the greening layout scheme into the numerical simulation software, simulations were conducted using the same boundary conditions and grid scheme as before optimization to ensure comparability and consistency of the simulation results. Subsequently, the wind speed field at the pedestrian breathing height of 1.5 m was obtained, as shown in the wind speed contour map in Figure 9. It can be observed that after introducing the greening layout strategy, trees have a positive impact on the wind environment of the block, while the proportion of green underlying surface and the green coverage rate have also been improved to some extent.

Comparing with the wind speed contour map before optimization, it can be seen that in the center of the block, i.e., the intersection area, wind speeds are significantly higher than the surrounding areas due to the building corner flow and the generated vortex zone. Between the two high wind speed surge zones, there is a leeward area formed by buildings blocking the incoming flow. In this area, wind speeds are relatively low, and the wind speed gradient with the surroundings is large, adversely affecting pedestrians' walking experience. After introducing the scheme, the area of the two high wind speed zones has been reduced, and the peak wind speed values have also decreased. The physical effect of buildings on wind speed is stronger than that of vegetation, so the high wind speed zone at the intersection is difficult to substantially mitigate through vegetation alone. Considering the aesthetic requirements of the block and the proportion of green underlying surface, vegetation layout cannot achieve full coverage and can only be locally fine-tuned.

In the northern section of the main street, there is also a large strong wind zone formed by the disturbed flow around buildings, with no vegetation arranged in the original environment. In this area with poor wind environment, frequent gusty weather could impair pedestrians' walking experience. After introducing the greening layout strategy, the extent of the strong wind zone in this area has been reduced, the wind speed gradient has become milder, and the gap between the upper and lower wind speed limits has narrowed, making the area suitable for dynamic activities such as walking and short-term standing rest. In the southern section of this street, most of the area falls within the pedestrian comfort wind speed range. Therefore, after introducing vegetation, while increasing the proportion of green underlying surface, the original wind speed range composition has not been significantly altered, and the area remains consistently within a pedestrian-friendly wind speed range.

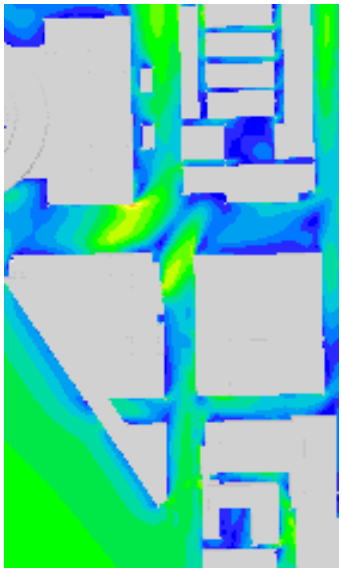

Figure 9. Simulated results after optimization

ISSN: 2472-3703 DOI: 10.6911/WSRJ.202605_12(5).0006

On the east-west oriented streets, except for the central intersection area, the overall wind speeds are lower than those on the north-south oriented streets. Therefore, a relatively conservative greening layout strategy was adopted. On the north-side east-west street, which faces the incoming wind direction, some of the original vegetation was replaced to reduce both the area of the strong wind zone when airflow enters the intersection and the upper threshold of wind speed. On the south-side east-west street, small trees were planted on one side of the crosswind zone to partially shrink the crosswind area while increasing the green coverage.

As shown in Figure 10, after introducing the greening layout strategy, the increases in the proportion of the comfortable wind speed range corresponding to each activity type are 3.37%, 8.70%, and -2.32%, respectively, while the overall increase in the proportion of the ideal wind speed area reaches 9.76%. Furthermore, in the uncomfortable moderate-to-high wind speed range of 5.01-10.7 m/s, the optimized block shows a reduction of 9.08% in the area proportion of this range. Since the introduction of greening spatial layout cannot have a positive optimization effect on all wind speed ranges, the optimization strategy aims to appropriately increase the area proportion of the 1.04-3.40 m/s range without excessively reducing the area proportion of the 3.41-5.00 m/s range.

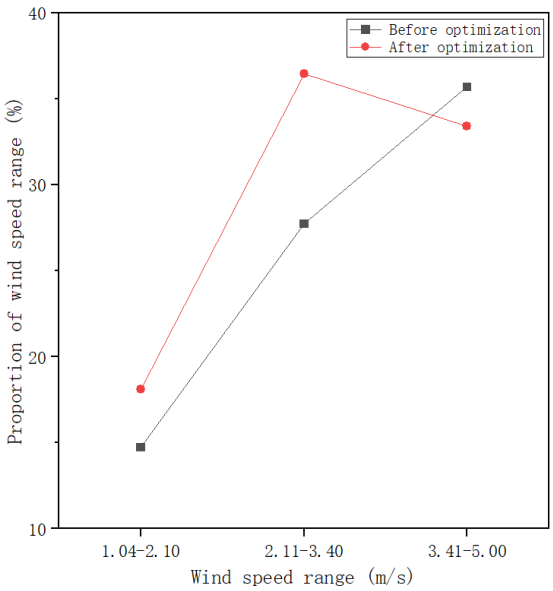

Figure 10. Comparison of area proportions of wind speed ranges before and after optimization

4.4. Optimization Strategy Recommendations

After the comprehensive optimization study of greening spatial layout in terms of space and plant characteristics, appropriate greening spatial layout strategies should be adopted according to the specific wind speed field within the block. If a large area of high wind speed exists in the block, two-sided planting can be used to control the wind speed. In blocks where localized high wind speed zones (crosswind zones, corner flow zones) coexist with low-speed leeward zones, single-row or central row planting may be considered. However, since central row planting may affect sightlines within the block, the strategy should be selected based on local conditions.

Furthermore, when selecting tree species for small and medium-sized trees, the principles of site-suitable tree selection and aesthetics should be followed. This section provides the following reference for suitable tree species, to help designers intuitively understand and

ISSN: 2472-3703 DOI: 10.6911/WSRJ.202605_12(5).0006

effectively apply the increase in green coverage and local microclimate optimization in commercial pedestrian streets.

Table 2. Recommended tree species

No.	Tree species
1	*Cinnamomum camphora* (L.) presl
2	*Koelreuteria bipinnata 'integrifoliola'* (Merr.) T.Chen
3	*Liquidambar formosana* Hance
4	*Ginkgo biloba* L.
5	*Sapindus Saponaria* Linnaeus
6	*Celtis julianae* C. K. Schneid. in Sarg.
7	*Platanus orientalis* L.
8	*Zelkova serrata* (Thunb.) Makino

5. CONCLUSIONS

Taking the core area of Hangzhou Hubin Pedestrian Street as a case study, addressing the two types of problems in the existing wind environment—strong wind discomfort zones and stagnant wind zones—this study carried out validation of greening layout optimization based on simulation results. According to the functional positioning and current wind environment of each zone, two-sided or single-sided row planting was adopted in zones A, B, and G, which are located on the incoming flow side or in areas with concentrated strong winds, to reduce high wind speeds. In zones E and F, where wind speeds are moderate, supplementary row planting was mainly used to balance green coverage and wind environment stability. In zones C and D, which are intersections and densely populated areas, no new trees were added to avoid disturbing the existing favorable wind environment. After optimization, the green coverage rate of the block increased from 1.70% to 5.90%, and the proportion of the ideal wind speed range (1.04-5.00 m/s) increased by 9.76 percentage points. Among this, the proportions of the 1.04-2.10 m/s and 2.11-3.40 m/s ranges increased by 3.37 and 8.70 percentage points, respectively, while the 3.41-5.00 m/s range decreased by only 2.32 percentage points. These results verify the effectiveness of the optimized greening spatial layout strategy in improving the wind environment of commercial pedestrian streets.

ACKNOWLEDGMENTS

The authors sincerely thank all colleagues and coauthors for their valuable contributions to this work.

REFERENCES

[1] Shao M.C., Hu W.J., and Dai Y.Z.: Research on Spatial Quality of Commercial Street Based on Street View Images: A Case Study of Quancheng Road and Shanshi East Road in Jinan, Urban Architecture, Vol.19 (2022) No.2, p.12-15.

[2] Li L.F.: *Research on Landscape Design of Urban Commercial Pedestrian Street* (MS., Soochow University, China 2012).

[3] Deng J.: *Study on the Correlation Between Urban Street Canyon Morphology and Microclimate and Optimization Strategies in Nanchang* (MS., Nanchang University, China 2024).

[4] Zhao Q. and Zhang T.: Integration of Evaluation Methods and Preliminary Strategies for Urban Outdoor Wind Environment, in *New Normal: Inheritance and Transformation – Proceedings of 2015*

ISSN: 2472-3703 DOI: 10.6911/WSRJ.202605_12(5).0006

China Urban Planning Annual Conference (07 Urban Ecological Planning) (Guiyang, China, 2015), p.215-229.

[5] Li P., Wang S., Wang Y.Y., et al.: The "Micro-Valley Effect" of Urban Road Green Belts and Its Impact on Pollutant Concentration on Non-motor Vehicle Lanes, Acta Ecologica Sinica, Vol.31 (2011) p.2888-2896.

[6] Tsang C.W., Kwok K.C.S., and Hitchcock P.A.: Wind Tunnel Study of Pedestrian Level Wind Environment Around Tall Buildings: Effects of Building Dimensions, Separation and Podium, Building and Environment, Vol.49 (2011) p.167-181.

[7] Guo M.M.: *Research on Spatial Form Optimization Strategies of Xi'an Tourism Commercial Pedestrian Street Based on Outdoor Human Comfort Improvement* (MS., Chang'an University, China 2022).

[8] Han J.: *Analysis and Optimization Strategies of Wind Environment in Kaifeng Old City Block* (MS., Henan University, China 2022).

[9] Zhu J.Q.: *Research on Spatial Form of Suzhou Commercial Pedestrian Street Based on Microclimate and Thermal Comfort* (MS., Suzhou University of Science and Technology, China 2022).

[10] Yang H. and Fu H.M.: Numerical Simulation and Experimental Study on Flow Resistance Characteristics of Tree Crowns, Journal of Central South University (Natural Science Edition), Vol.47 (2016) No.12, p.4292-4300.

[11] Zeng F.H.: *Influence of Spatial Layout Pattern of Road Green Belt on Airflow Characteristics in Typical Street Canyons* (MS., Zhejiang A&F University, China 2022).

[12] Shen X.Y.: *Influence of Spatial Distribution of Trees on Airflow Inside Typical Street Canyons* (MS., Fuzhou University, China 2018).

[13] Li Y.C.: *Research on the Spatial Layout of Greenery in Pedestrian Streets Oriented by Good Ventilation Environment* (MS., Chongqing University, China 2020).

[14] Gu L.L.: *Study on the Correlation Between Air Quality Improvement and Spatial Form of Plazas in Urban Central Area* (MS., Chongqing University, China 2018).

[15] Zhao H.Y.: *Influence of Canopy Spatial Characteristics of Street Trees on Wind Environment in Shallow Street Canyons* (MS., Zhejiang A&F University, China 2024).

[16] Jiang Y.F.: Urban Renewal Aiming at Improving the Quality of Human Settlement Space – Taking Sanxia Square Commercial Pedestrian Street as an Example, in *Beautiful China, Co-construction, Co-governance and Sharing – Proceedings of 2024 China Urban Planning Annual Conference (03 Urban Renewal)* (Hefei, China, 2024), p.3207-3226.

[17] Xiang N.: *Research on Wind Environment Evaluation and Design Strategies of Jinan Historical Commercial Pedestrian Street* (MS., Shandong Jianzhu University, China 2022).

[18] Zhao J.Y. and Liu J.P.: Dynamic Thermal Effect of Greening in Urban Street Canyons, Acta Energiae Solaris Sinica, Vol.30 (2009) No.8, p.1013-1017.